

Aperiodic fragments in periodic solids: Eliminating the need for supercells and background charges in electronic structure calculations of defects

Robert H. Lavroff,¹ Daniel Kats,² Lorenzo Maschio,³ Nikolay Bogdanov,²
Ali Alavi,⁴ Anastassia N. Alexandrova,⁵ and Denis Usvyat^{6,*}

¹*Department of Chemistry and Biochemistry, University of California Los Angeles, Los Angeles, California, USA*

²*Max Planck Institute for Solid State Research, Heisenbergstraße 1, D-70569 Stuttgart, Germany*

³*Dipartimento di Chimica, Università di Torino, Torino, Italy*

⁴*Max Planck Institute for Solid State Research, Heisenbergstraße 1,
D-70569 Stuttgart, Germany and Yusuf Hamied Department of Chemistry,
University of Cambridge, Lensfield Road, Cambridge CB2 1EW, United Kingdom*

⁵*Department of Chemistry and Biochemistry, University of California Los Angeles,
Los Angeles, California, USA; Department of Materials Science and Engineering,
University of California Los Angeles, Los Angeles, California,*

USA; and California Nanoscience Institute (CNSI), Los Angeles, California, USA

⁶*Institut für Chemie, Humboldt-Universität zu Berlin, Brook-Taylor-Str. 2, D-12489 Berlin, Germany*

(Dated: June 6, 2024)

To date, computational methods for modeling defects (vacancies, adsorbates, etc.) rely on periodic supercells in which the defect is far enough from its repeated image such that they can be assumed non-interacting. Defects in real solids, however, can be spaced microns or more apart, whereas affordable supercells for density functional theory calculations are no wider than a few nanometers. The relative proximity and periodic repetition of the defect's images may lead to spurious unphysical artifacts, especially if the defect is charged and/or open-shell. Furthermore, to avoid divergence of the periodic electrostatics, a compensating background charge must be introduced if the defect is charged. Even if post-hoc corrections are used, this is a source of unquantifiable error and, in some cases, renders total energies and energy differences useless. In this communication, we introduce a "defectless" embedding formalism such that a pristine, primitive unit cell may be used for the periodic mean field, after which atoms may be moved or charged within an embedded fragment. This fragment can then be treated with a post-Hartree Fock method to capture important electron correlations pertaining to the defect. By eliminating the need for compensating background charges and periodicity of the defect, we circumvent all associated unphysicalities and numerical issues. Furthermore, the primitive cell calculations drastically reduce computational expense compared to supercell approaches. This embedded aperiodic fragment approach is size-intensive with respect to energy differences and can be routinely applied even to multireference defects, localized excited states, etc. using a variety of fragment solvers. In examining with this approach bond-breaking in a fluorine-substituted graphane monolayer, a difficult testing ground for condensed-phase electronic structure methods, we observe key aspects of the dissociation pathway, specifically a covalent-to-ionic avoided crossing.

INTRODUCTION

Due to its accuracy relative to computational cost, Kohn-Sham density-functional theory (DFT) has become the workhorse of computational materials study. DFT is not, however, a systematically improvable method due to lack of knowledge of the exact exchange-correlation functional, making it impossible to guarantee approaching an exact description. Wavefunction-based quantum chemistry, by contrast, does systematically approach exact solutions via hierarchies of increasingly accurate methods. Hartree-Fock (HF) theory is the "lowest rung" of all these hierarchies, which lacks any description of electron correlation aside from Fermi correlation, the mere enforcing of the Pauli exclusion principle by preventing any two electrons from occupying the same spatial and spin state at once. From here, a post-HF treatment can be applied to include electron correlations beyond Fermi correlation. These post-HF methods, however,

scale rapidly with system size, making their application to extended systems without additional (sometimes drastic) approximations difficult. Nonetheless, wavefunction-based methods have become relatively commonplace for periodic systems in recent decades, whether with actual periodic techniques[1–20] or the so-called method of increments[21–26] and other approaches combining periodic and finite-cluster calculations[27–37]. Such techniques, however, have been nearly exclusively applied for closed-shell systems and their generalization to capture multireference character (strong electron correlation) is difficult.

If strong correlation is localized to a particular site on a crystal or surface, such as a defect, a natural approach is to introduce an embedded fragment in which a portion of the system is treated with an accurate post-HF method while the surroundings are characterized with a periodic mean field-method such as HF or DFT. A variety of these embedding schemes have been developed[38–

98], based in the density, density matrix, Fock matrix, or Green's function/self-energy, some of which can treat both ground and excited states. Particularly relevant to this work are periodic Hartree-Fock embedding schemes [99–107]. Thus far, however, all embedding approaches that involve periodic treatment share the same two major drawbacks. First, the site with strong correlation, which will inherently have different geometry than the rest of the system, must be present during the periodic mean-field calculation as well as the post-HF fragment calculation. This means that the defect is infinitely and periodically repeated, and the periodic unit chosen must be a large supercell such that the correlated site is far enough from its repeated images. This often leads to high computational expense for the periodic treatment of the system, and the need for post-hoc corrections due to possible interaction[108] further complicates the situation. Second, in periodic boundary conditions, a non-neutral unit repeating infinitely causes the Coulomb potential of the system to diverge. Thus, if the strongly correlated site is charged (e.g. an anionic or cationic vacancy), a compensating background charge must be used to make the overall cell neutral. This artificial charge, implemented in practice by throwing away a diverging term in the momentum-space expansion of the Coulomb potential, causes total energy to depend strongly on the size of the vacuum in the case of a molecule, polymer, or slab (i.e. anything but a bulk crystal) in a plane wave basis[109–111]. This makes total energies useless and untrustworthy to determine relative energies. Even in the case of a Gaussian basis for periodic systems, where a vacuum is not required, this compensating background charge is an artifact and a source of unquantifiable error. Pure finite-cluster approaches, possibly embedded in point charges, on the other hand do allow for a multireference treatment of radical or charged defects [112–119]. However, the ambiguity of the embedding parameterization and sensitivity of clusters to bond cutting compromises the accuracy and transferability of such schemes.[120]

In this study, we present an embedded fragment formulation which alleviates these issues by allowing movement of fragment nuclei and change of the fragment charge *after* the periodic HF calculation. In this way, the periodic mean field, serving as the embedding field for the fragment, may be calculated using the primitive cell with no defects. This pristine periodic calculation not only saves computational time by circumventing a supercell, but also allows for fragments to be embedded in the defect-free, mean-field embedding potential. Smaller unit cells additionally allow for state-of-the-art electron correlation methods[121, 122] which closely approach exact diagonalization (full configuration interaction). This embedding scheme also includes a possibility for a charged fragment without compensating background charges, as the fragment itself is not periodically repeated. As shown in our calculations and discussion, aperiodic embedding allows

for routine calculations of multireference sites in nonconducting periodic systems.

THEORY

Fragment embedded in periodic HF without introduction of a defect

Our analysis begins with a model of a crystal's fragment, defined in terms of local orbitals, electrons, and nuclei, embedded in the mean field of the rest of the crystal. At this point, we keep the geometry of the fragment unaltered, which we will refer to as a frozen fragment. It corresponds to a mere partitioning of the crystalline space into a fragment and the embedding environment. This setup is similar to that of the embedded fragment model of Refs. 102, 103, and 106; however, there are a few important distinctions. First, the standard fragment approach restricts the orbital space exclusively for the post-HF treatment on top of the full periodic HF. Here, in contrast, the treatment of the embedded fragment starts already at the HF stage. Second, the fragment's nuclei are not only centers for the basis orbitals, as in the standard approach, but also hold the actual nuclear charges. In this way the overall problem is formulated not just as a frozen-environment approximation for the post-HF treatment, but rather as the HF and post-HF description of a physical fragment embedded in the periodic environment.

The one-electron Hamiltonian of a frozen fragment

Despite the difference in the model, without a change in the fragment geometry, the one-electron Hamiltonian $h^{\text{frozen frag}}$ of the present embedded fragment approach is equivalent to the standard one introduced e.g. in Ref. [106]. For simplicity we consider a closed-shell crystal and a closed-shell fragment:

$$\begin{aligned}
 h_{\mu\nu}^{\text{frozen frag}} &= \left\langle \mu \left| -\frac{1}{2}\nabla^2 \right| \nu \right\rangle + \left\langle \mu \left| -\sum_K \frac{Z_K}{|\mathbf{r} - \mathbf{R}_K|} \right| \nu \right\rangle \\
 &+ \sum_{i \notin \text{frag}} [2(\mu\nu|ii) - (\mu i|i\nu)] \\
 &= F_{\mu\nu}^{\text{per}} - \sum_{i \in \text{frag}} [2(\mu\nu|ii) - (\mu i|i\nu)], \quad (1)
 \end{aligned}$$

where μ, ν, \dots are some local basis functions, i – localized occupied orbitals of the converged periodic HF solution, F^{per} is the periodic Fock matrix, and the electron repul-

sion integrals (ERIs) are given in the chemical notation:

$$(\mu\nu|\rho\sigma) = \int d\mathbf{r}_1 d\mathbf{r}_2 \phi_\mu^*(\mathbf{r}_1) \phi_\nu(\mathbf{r}_1) \frac{1}{|\mathbf{r}_1 - \mathbf{r}_2|} \phi_\rho^*(\mathbf{r}_2) \phi_\sigma(\mathbf{r}_2). \quad (2)$$

It is evident that the fragment's one-electron Hamiltonian (eq. 1) contains the Coulomb and exchange potential from the electrons of the environment and the external potential from the nuclei of both fragment and environment. In the frozen fragment model, the fragment's nuclei are a subset of the nuclei of the periodic solid, so their contribution is included in the periodic Fock matrix.

HF energy of a frozen fragment

For the HF energy, the equivalence between the standard embedded-fragment model[102, 106] and the model of an aperiodic fragment no longer holds, even if the aperiodic fragment is frozen. In the former model, the fragment HF *was chosen* to coincide with the periodic HF energy per cell. In the model developed in the current work, the actual HF energy of the physical fragment subjected to embedding is considered. That is, the HF energy of the isolated fragment plus the energy of the interaction between the fragment and the environment:

$$\begin{aligned} E_{\text{HF}}^{\text{frozen frag}} &= 2 \sum_{i \in \text{frag}} \left\langle i \left| -\frac{1}{2} \nabla^2 \right| i \right\rangle - 2 \sum_{i \in \text{frag}} \left\langle i \left| \sum_{K \in \text{frag}} \frac{Z_K}{|\mathbf{r} - \mathbf{R}_K|} \right| i \right\rangle + \frac{1}{2} \sum_{i \in \text{frag}} \sum_{j \in \text{frag}} [4(ii|jj) - 2(ij|ji)] \\ &+ \frac{1}{2} \sum_{L \in \text{frag}} \sum_{K \in \text{frag}} \frac{Z_L Z_K}{|\mathbf{R}_L - \mathbf{R}_K|} - 2 \sum_{i \notin \text{frag}} \left\langle i \left| \sum_{K \in \text{frag}} \frac{Z_K}{|\mathbf{r} - \mathbf{R}_K|} \right| i \right\rangle - 2 \sum_{i \in \text{frag}} \left\langle i \left| \sum_{K \notin \text{frag}} \frac{Z_K}{|\mathbf{r} - \mathbf{R}_K|} \right| i \right\rangle \\ &+ \sum_{i \in \text{frag}} \sum_{j \notin \text{frag}} [4(ii|jj) - 2(ij|ji)] + \sum_{L \notin \text{frag}} \sum_{K \in \text{frag}} \frac{Z_L Z_K}{|\mathbf{R}_L - \mathbf{R}_K|}. \end{aligned} \quad (3)$$

The first four terms in eq. (3) form the HF energy of an isolated fragment; the 5th and 6th terms give the energy of the Coulomb attraction between the electrons or nuclei of the environment and nuclei or electrons of the fragment, respectively; the 7th term is the Coulomb and exchange contributions due to the interaction between the electrons of the environment and the fragment; and finally the 8th term is the Coulomb repulsion between the nuclei of the environment and the fragment.

By noting that the terms 2, 4 (taken twice), 5 and 8 together can be rewritten via the electrostatic potential of

the periodic system $V(\mathbf{r})$ at the locations of the fragment nuclei:

$$\begin{aligned} &Z_K \left[-2 \sum_i \left\langle i \left| \frac{1}{|\mathbf{r} - \mathbf{R}_K|} \right| i \right\rangle + \sum_L \frac{Z_L}{|\mathbf{R}_K - \mathbf{R}_L|} \right] \\ &= Z_K \cdot V(\mathbf{R}_K) \end{aligned} \quad (4)$$

and regrouping other terms, one can simplify expression (3):

$$\begin{aligned} E_{\text{HF}}^{\text{frozen frag}} &= 2 \sum_{i \in \text{frag}} h_{ii}^{\text{frozen frag}} + \sum_{i \in \text{frag}} \sum_{j \in \text{frag}} [2(ii|jj) - (ij|ji)] \\ &+ \sum_{K \in \text{frag}} Z_K \cdot V(\mathbf{R}_K) - \frac{1}{2} \sum_{K \in \text{frag}} \sum_{L \in \text{frag}} \frac{Z_K Z_L}{|\mathbf{R}_K - \mathbf{R}_L|} + 2 \sum_{i \in \text{frag}} \left\langle i \left| \sum_{K \in \text{frag}} \frac{Z_K}{|\mathbf{r} - \mathbf{R}_K|} \right| i \right\rangle \\ &= \frac{1}{2} \sum_{i \in \text{frag}} [2h_{ii}^{\text{frozen frag}} + 2F_{ii}^{\text{frozen frag}}] + E_{\text{nuc}}^{\text{frozen frag}}. \end{aligned} \quad (5)$$

This shows that the HF energy of the frozen embedded fragment can be defined via the fragment one-electron

Hamiltonian (1), fragment Fock matrix:

$$\begin{aligned} F_{\mu\nu}^{\text{frozen frag}} &= h_{\mu\nu}^{\text{frozen frag}} \\ &+ \sum_{i \in \text{frag}} \sum_{i \in \text{frag}} [2(\mu\nu|ii) - (\mu i|i\nu)] \end{aligned} \quad (6)$$

and an effective ‘‘nuclear energy’’

$$E_{\text{nuc}}^{\text{frozen frag}} = \sum_{K \in \text{frag}} Z_K \cdot V(\mathbf{R}_K) - \frac{1}{2} \sum_{K \in \text{frag}} \sum_{L \in \text{frag}} \left[\frac{Z_K Z_L}{|\mathbf{R}_K - \mathbf{R}_L|} + 2 \sum_{i \in \text{frag}} \left\langle i \left| \sum_{K \in \text{frag}} \frac{Z_K}{|\mathbf{r} - \mathbf{R}_K|} \right| i \right\rangle \right] \quad (7)$$

Fragment with explicitly introduced defect

Now we introduce a defect in the fragment by removing, adding, and/or substituting nuclei in the fragment accompanied by a respective update of the number of electrons (though we re-emphasize that the fragment need not be neutral; the number of electrons can be altered to produce a cationic or anionic fragment). We will refer to a fragment with this modification as an aperiodic defect, because its structure is not repeated into the environment.

To distinguish the atoms and orbitals of the aperiodic defect their indices will be decorated with a prime, as opposed to the ‘‘un-primed’’ indices denoting atoms and orbitals prior to the fragment structure manipulation. For the indices of the fragment nuclei:

$$\begin{aligned} K \in \text{frag} &\rightarrow K' \in \text{frag} \\ R_K|_{K \in \text{frag}} &\rightarrow R_{K'}|_{K' \in \text{frag}} \\ Z_K|_{K \in \text{frag}} &\rightarrow Z_{K'}|_{K' \in \text{frag}} \end{aligned}$$

This will also be the case for the new occupied i' , j' , ... and the virtual a' , b' , ... orbitals of the fragment, coming from the fragment’s self-consistent field (SCF), as the initial periodic HF orbitals will no longer be solutions of the fragment’s HF calculation.

Importantly, both occupied and virtual orbitals of the fragment ψ'_i and ψ'_a must remain orthogonal to the frozen occupied orbitals of the environment $\psi_i \notin \text{frag}$, as otherwise the electron number conservation cannot be guaranteed. We preserve this orthogonality at level of fragment’s basis orbitals μ' , obtained by projecting the AOs of the fragment atoms from the occupied space of the environment:

$$|\mu'\rangle = \left(1 - \sum_{i \notin \text{frag}} |i\rangle \langle i| \right) |\mu\rangle \quad (8)$$

The fragment’s basis orbitals μ' are centered on the nuclei after the structure modification K' . Such a choice of the

basis by construction guarantees the orthogonality of the fragment orbitals to the environment.

One electron Hamiltonian of aperiodic fragment

If the geometry has been manipulated, the potential energy operator must be updated. Adding the corresponding correcting terms to eq. (1) yields for the one electron operator of the aperiodic defect h^{defect} :

$$\begin{aligned} h_{\mu'\nu'}^{\text{defect}} &= h_{\mu'\nu'}^{\text{frozen frag}} + \left\langle \mu' \left| \sum_{K \in \text{frag}} \frac{Z_K}{|\mathbf{r} - \mathbf{R}_K|} \right| \nu' \right\rangle \\ &\quad - \left\langle \mu' \left| \sum_{K' \in \text{frag}} \frac{Z_{K'}}{|\mathbf{r} - \mathbf{R}_{K'}|} \right| \nu' \right\rangle \end{aligned} \quad (9)$$

The summation $\sum_{K \in \text{frag}}$ in (9) goes over the fragment atoms of the initial structure, while the one $\sum_{K' \in \text{frag}}$ over those in the new one. The Fock matrix of the aperiodic defect is naturally defined as:

$$\begin{aligned} F_{\mu'\nu'}^{\text{defect}} &= h_{\mu'\nu'}^{\text{defect}} \\ &\quad + \sum_{i' \in \text{frag}} [2(\mu'\nu'|i'i') - (\mu'i'|i'\nu')] \end{aligned} \quad (10)$$

If no geometry modification has been performed, the h^{defect} and $F_{\mu'\nu'}^{\text{defect}}$ reduce to $h_{\mu'\nu'}^{\text{frozen frag}}$ and $F_{\mu'\nu'}^{\text{frozen frag}}$, respectively.

HF energy of aperiodic fragment

The fragment structure must also be modified to include (i) the change in the position of the nuclei and (ii) the new fragment orbitals as the HF solutions:

$$\begin{aligned} E_{\text{HF}}^{\text{defect}} &= \frac{1}{2} \left(\sum_{i' \in \text{frag}} [2h_{i'i'}^{\text{defect}} + 2F_{i'i'}^{\text{defect}}] \right) \\ &\quad + E_{\text{nuc}}^{\text{defect}}, \end{aligned} \quad (11)$$

with the effective $E_{\text{nuc}}^{\text{defect}}$:

$$\begin{aligned}
E_{\text{nuc}}^{\text{defect}} = & \frac{1}{2} \sum_{K' \in \text{frag}} \sum_{L' \in \text{frag}} ' \frac{Z_{K'} Z_{L'}}{|\mathbf{R}_{K'} - \mathbf{R}_{L'}|} + \sum_{K' \in \text{frag}} Z_{K'} \cdot V(\mathbf{R}_{K'}) \\
& + 2 \sum_{i \in \text{frag}} \left\langle i \left| \sum_{K' \in \text{frag}} \frac{Z_{K'}}{|\mathbf{r} - \mathbf{R}_{K'}|} \right| i \right\rangle - \sum_{K \in \text{frag}} \sum_{K' \in \text{frag}} ' \frac{Z_K Z_{K'}}{|\mathbf{R}_K - \mathbf{R}_{K'}|}. \quad (12)
\end{aligned}$$

The first of these terms is merely the energy of the clamped nuclei at the new position. The second is the complete electrostatic potential from the previous geometry (from both electrons and nuclei, and from both the old positions of fragment's nuclei and from the frozen environment) at the new positions of the nuclei. The third is for cancellation of the interaction from the fragment electrons in the previous geometry, and the fourth is for cancellation of the interaction from the displaced nuclei of the previous geometry. The second, third, and fourth terms constitute the electrostatic potential from the frozen environment. In the case where the entire system is encompassed by the fragment and there is no environment, the three will sum to zero and the $E_{\text{HF}}^{\text{defect}}$ will take the usual expression of molecular RHF. In case of unmodified embedded fragment, it instead reduces to $E_{\text{HF}}^{\text{defect}}$ of eq. (3).

Like in eq. (9), the summations over K and K' in (12) are performed over the fragment nuclei before and after formation of the defect, respectively. However, it is neither necessary to include the unaltered fragment nuclei (i.e. when $K=K'$) in (9) nor in (12). As demonstrated in SI, section S2.1, inclusion of such atoms in the fragment is irrelevant for energy differences, as they add only a constant shift to the defect's HF energy.

As a side note, the embedded frozen fragment HF energy (3) is not size-extensive in the sense that the HF energy of a fragment coinciding with two unit cells is not twice the HF energy of a one-unit-cell fragment. However, for application of the aperiodic fragment approach, the essential property is asymptotic intensivity of the energy differences. It is shown in SI section S2.2, that this property is indeed fulfilled, which demonstrates that the physically relevant quantities in our approach are well defined, making it useful for real systems.

Implementation

The implementation of the embedded aperiodic fragment involves a consecutive run of several programs. First, a primitive unit-cell periodic HF calculation, and localization of the occupied orbitals is done via the Crystal code [123]. In these calculation the new positions of the atoms of the defect are occupied by ghost "placeholders" that contain no charge and an ultra-narrow s-AO with a large Gaussian exponent (1,000,000 au) such that no electron can actually occupy it. Crystal also evalu-

ates the electrostatic potential $V(\mathbf{R}_{K'})$ at the position of the manipulated atoms K' . Next, in a second, single-iteration run of the Crystal code, the actual AOs are added on the placeholder centers in order to evaluate the Fock matrix in the basis of these AOs.

This information is transferred to the Cryscor code [103], which is used to define the fragment in terms of atoms K and K' , fragment AOs $\mu \in \text{frag}$, and occupied orbitals $i \in \text{frag}$. Once the fragment is defined, its basis functions are constructed according to eq. (8).

The in-fragment HF treatment, which is described in detail in the SI, is based on density fitting approach and involves only 3-index quantities $B_{\mu'\nu'}^P$:

$$B_{\mu'\nu'}^P = \sum_Q (\mu'\nu'|Q) [J^{-1/2}]_{QP}, \quad (13)$$

with $J_{PQ} = (P|Q)$. Here P, Q denote the fitting functions from the auxiliary basis. Calculation of the fragment's one-electron Hamiltonian (1) requires additional quantities $B_{i\nu'}^P$ and B_{ii}^P , which are defined analogously to $B_{\mu'\nu'}^P$. The 2- and 3-index two-electron integrals, as well as the B s, are calculated using the machinery of Cryscor's periodic local density fitting [124].

After the SCF has converged, one can readily perform post-HF treatment (single- or multireference) via the FCIDUMP interface [125]. For this, we assemble the 4-index integrals from the 3-index quantities $B_{\mu'\nu'}^P$ transformed to the basis of active orbitals. The FCIDUMP interface can be used by a number of molecular codes. In this work, we use Molpro [126]. Figure 1 outlines this workflow and how it compares to that of the embedding scheme of Ref [106].

CALCULATIONS AND DISCUSSION

Since the method is based on partitioning of the space with localized occupied orbitals, like many quantum embedding schemes, it cannot yet be used to reliably study conducting solids. As a test system, we have taken graphane, which is 2D-periodic and nonconducting, with a substitution of a hydrogen atom with fluorine (henceforth referred to as fluorographane). The technical details of the calculations are outlined in SI Section 3, while the aperiodic fragment is shown in Figure 2.

Fluorographane is a convenient testbed for our method, and for defects in general, as it has a substan-

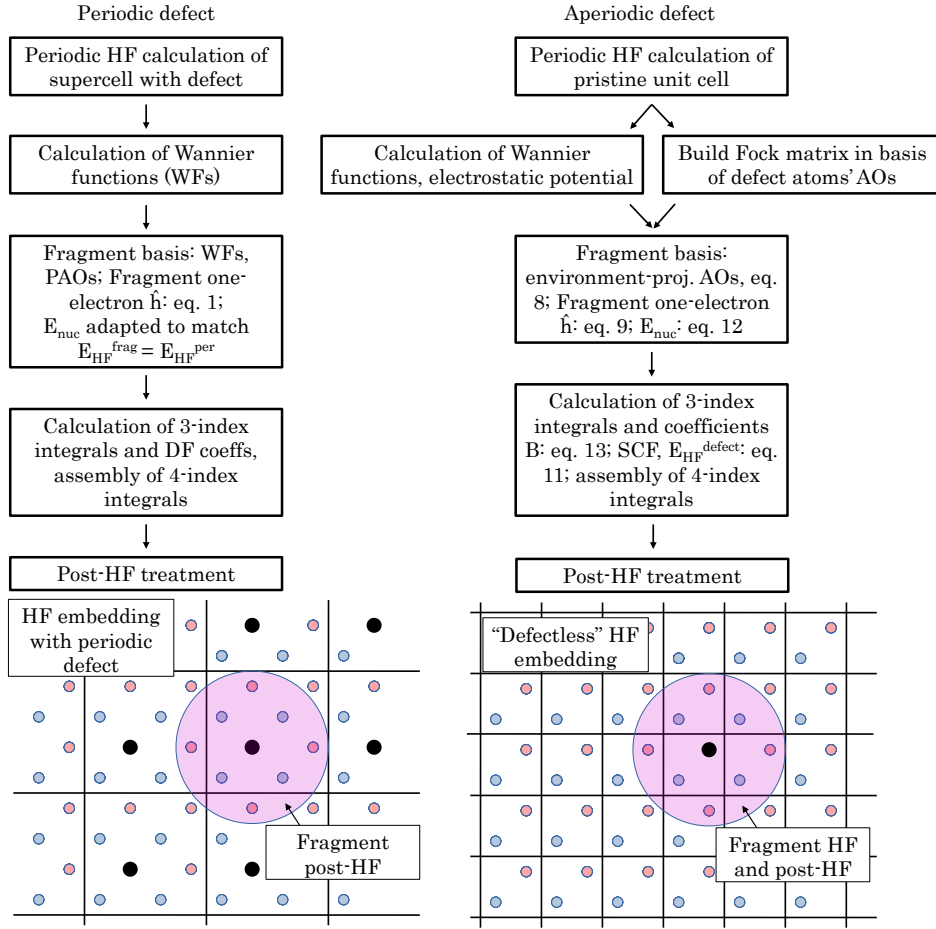


FIG. 1. Flowcharts and schematics outlining the workflows of the embedded periodic defect of Ref. [106] (left) and the embedded aperiodic defect presented here (right).

tial amount dynamic correlation due to the presence of valence-electron-rich fluorine, and, at the same time, one can tune the amount of static correlation (similar to increasing the U parameter in a Hubbard model) by a gradual, homolytic dissociation of the fluorine atom. Systems with both dynamic (weak) and static (strong) correlation, a situation common for defects, are generally difficult for electronic structure theory. DFT is, in principle, able to describe weakly correlated systems, but as mentioned above, the actual level of accuracy is difficult to assess a-priori. For strongly correlated systems, DFT may fail even qualitatively. Quantum chemical single-reference methods, while adept at treating dynamic correlation with systematic improvability also fail for static correlation (with rare exceptions). Multireference methods capture static correlation, but generally struggle to affordably treat dynamic correlation.

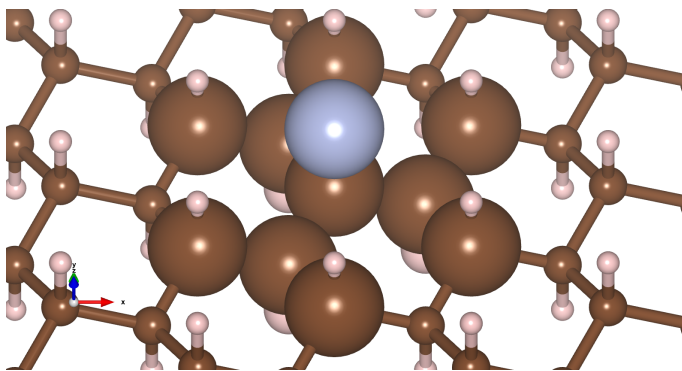


FIG. 2. Visualization of the aperiodic fluorographane fragment and environment at its equilibrium bond length. The fragment is shown as space filling (noting that three hydrogen atoms on the underside of the monolayer are included), while the environment is shown as "ball-and-stick." Carbon atoms are brown, hydrogen atoms are pink-white, and the fluorine atom is pale blue.

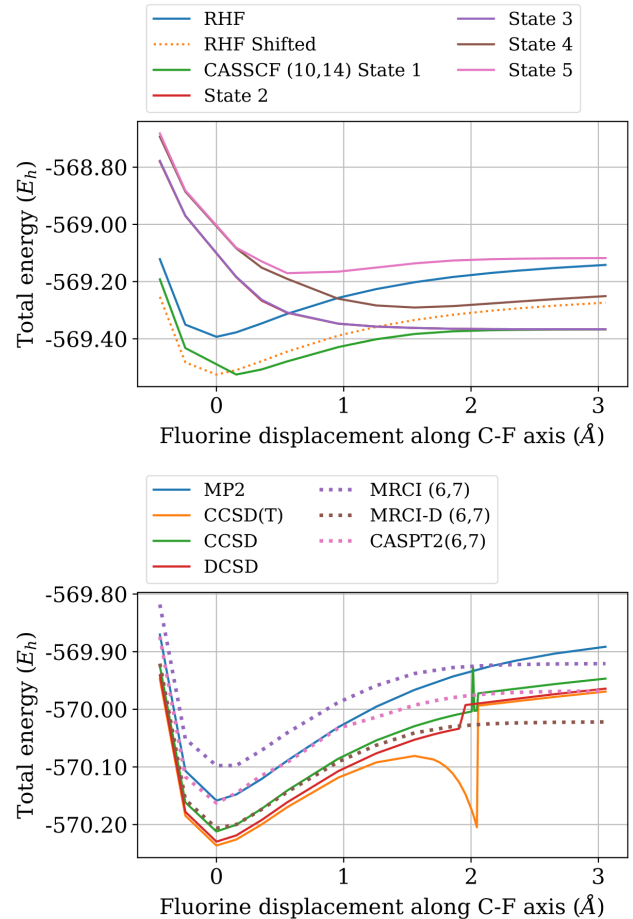


FIG. 3. Potential energy curves for a single fluorine atom dissociation in a fluorine-hydrogen substitution defect in graphane using the aperiodic fragment approach. Top: RHF, energy-shifted RHF and SA(5)-CASSCF(10,14) with 5 lowest singlet states. States 2 and 3 are degenerate along the entire curve, and the avoided crossing occurs between states 1 and 4. Bottom: Methods which include dynamical correlation applied to the same potential energy curves (ground state only): MRCI, MRCI with Davidson correction, CASPT2 (all with (6,7) active space), MP2, DCSD, CCSD and CCSD(T). Results of single-reference methods are shown with solid lines; those of multireference methods are shown with dashed lines.

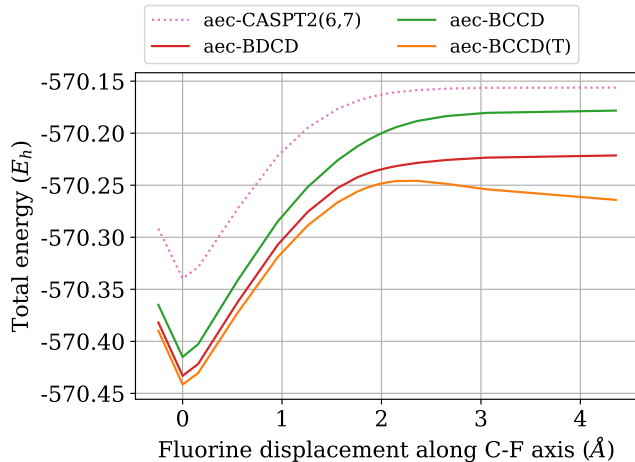


FIG. 4. BDCD, BCCD, BCCD(T) and CASPT2 (6,7) potential energy curves for a single fluorine atom dissociation in a fluorine-hydrogen substitution defect in graphane using the aperiodic fragment approach. "aec" stands for "all-electron correlated"; all Brueckner and CASSCF orbitals are re-optimized at each geometry with the orbitals from the previous geometry taken as starting guess, so the frozen-core approximation is not employed.

We start our analysis with the RHF and CASSCF results shown at the top panel of Figure 3. Neither of these methods include dynamic correlation, but CASSCF can capture static correlation and also be used for excited states. The RHF curve, although reasonable near the minimum, sticks to the incorrect ionic dissociation, as is actually expected from this method. Qualitatively, it is similar to the periodic HF curve of the supercell approach (Fig. 2 of Ref. [106]), but slightly less steep. The reason for an additional steepness in the supercell model is not just one fluorine atom is dissociated, but a sparse fluorine monolayer (one atom per supercell), which adds an additional (and unphysical) energy penalty.

The CASSCF curves, despite the lack of dynamic correlation, describe the neutral dissociation qualitatively correctly. Moreover, with CASSCF, the whole landscape of the local excited states can be reconstructed. In this system, it demonstrates the avoided crossing between states 1 and 4 and the switch of dissociative ground state character from ionic to neutral at about 1.5 Å of the bond elongation. This same crossing is shown to be present in fluoromethane (SI Figure 2).

The bottom panel of Figure 3 compiles the methods that include dynamic correlation. Firstly we note that the multireference methods, MRCI [127, 128], MRCI-D (i.e. MRCI with Davidson's size-extensivity correction), and CASPT2[129], correct the CASSCF bond length minimum, showing the importance of dynamic correlation. As expected, they also correctly describe the neutral dissociation limit. The single reference methods tested here all mutually agree near the minimum. All

of them reproduce the ionic dissociation, however. MP2 follows HF and stays on the ionic state along the whole dissociation curve. Distinguishable cluster singles and doubles (DCSD) [130] and CCSD do switch to the neutral state at the avoided crossing point, but very soon become unstable due to the growth of static correlation in this state. This growth is evident from the divergent behaviour of the perturbative triples contribution, (T). At some point (near 2 Å of the bond elongation), all these methods switch to the ionic state.

The problem of instability of DCSD method at fluorine dissociation is somewhat curious, as it is known to be capable of dealing with static correlation better than most single-reference methods [131]. In order to investigate this, in Figure 4, we employ Brueckner distinguishable cluster doubles (BDCD) [132] along with Brueckner coupled cluster doubles (BCCD) [133, 134], BCCD(T), and CASPT2 as a reference. To facilitate stability, the starting guesses for Brueckner orbitals along the dissociation path were taken from the previous geometries. In order to keep the order of orbitals from one point to another, the FCIDUMP was written directly in the (symmetrically orthogonalized) basis orbitals μ' . In contrast to DCSD, BDCD is indeed very stable along the whole dissociation and fairly well reproduces the CASPT2 reference with only a slight overestimation of the dissociation energy. BCCD does not break down either, but its dissociation energy is much larger than CASPT2's. Finally, the (T) correction exhibits its trademark asymptotic divergence in the presence of strong correlation.

With these results at hand, we point out the major differences between aperiodic embedding and the standard supercell approach. Apart from substantial efficiency gains at the periodic part of the calculation, aperiodic embedding offers also conceptual advantages. The unphysical periodization of a strongly correlated defect can influence the accuracy of the calculation in multiple ways. It may have a negative impact on the periodic HF contribution, the embedding field, fragment orbital space, etc. The aperiodic embedding explicitly deals with a single defect and thus is free of these issues. In our system, for example, the supercell approach of Ref. [106] led to an effective breaking of an infinite number of bonds at once, i.e. dissociating a sparse fluorine monolayer from the graphane surface. Even within the ionic dissociation reproduced by HF, the interaction was enhanced and the static correlation increased, as suggested by the divergence of the supercell MP2 curve. Furthermore, periodic HF and localization procedures were becoming progressively unstable with dissociation, effectively prohibiting the use of the periodic fragment approach beyond 2 Å of bond elongation. With the aperiodic fragment method, the periodic HF is unproblematic and corresponds to the well-behaved, closed-shell, non-defective system regardless of the a-posteriori bond elongation distance. Again, only one bond is dissociated,

preventing unintended sources of strong correlation beyond the defect itself. This stark contrast shows the importance of using aperiodicity (or possibly a much larger and very expensive supercell) for strong correlation (i.e. bond breaking) in solids. Demonstration of the other key advantage of aperiodic embedding, realistic treatment of charged defects, will be shown in a forthcoming, additional publication.

CONCLUSIONS

In this communication, we have introduced a quantum embedding scheme for an "aperiodic" fragment embedded in the "defectless" periodic HF solution, eliminating the need for periodic repetition of the defect and associated expensive supercells, compensating background charges, and associated charge corrections in electronic structure calculations of solid-state defects. An aperiodic fragment containing the defect is placed in a frozen environment of the periodic Hartree Fock solution calculated using pristine, minimal unit cells, leading to significant computational savings and reduced approximations. The only required assumption is that the fragment is large enough to capture the electronic structure of the defect, which can be confirmed with simple benchmarking and possibly extrapolation.

While we formulate this approach in the context of periodic Hartree Fock embedding, it can be readily extended to other mean-field approaches. HF embedding with DFT orbitals is possible right away without any additional implementation efforts. A proper DFT embedding would require calculation of the integrals for the exchange-correlation potential, but otherwise very little effort (Fock exchange would merely be supplemented or replaced by exchange-correlation). This, however, may lead to double-counting of dynamical correlation in the embedded fragment, for which a correction term would likely need to be derived.

Another important extension of the scheme is a possibility to reach self-consistency between fragment and environment. Formation of a defect, especially if the defect is not neutral, can trigger a response from the environment, which in turn can influence the electronic structure of the fragment. At the moment this effect can be taken into account by expansion of the fragment with a subsequent extrapolation. Incorporation of the explicit Coulomb response of the environment [67] will substantially speed up the convergence with fragment size and thus allow for high accuracy already with modest-sized fragments. Transcorrelation approaches[135, 136] could also assist in alleviating these finite size effects, as well as basis set error and overall accuracy. Further useful development avenues include local correlation treatment for the fragment and possibly environment. One can envision using local many-body perturbation theory or cou-

pled cluster theory for the environment, where the fragment's amplitudes or Hamiltonian would be coupled to or "dressed with" the amplitudes of the environment. Analytic gradients and higher-order energy derivatives would also prove useful, for example in geometry optimization of the fragment.

Finally, a question of future interest is whether this approach could be reliably extended to metallic solids. The most glaring issue here is the delocalized nature of metallic electrons, making it difficult, but not impossible[137], to localize them into fragments and Wannier functions (WFs). Non-particle-conserving mean-field theories[138, 139] and/or non-one-to-one correspondence between bands/Bloch states and WFs[140] show potential for this extension to metals. Transcorrelation has also been shown to allow methods typically divergent for gapless systems to readily be used on metals and is thus promising for this goal [141].

SUPPLEMENTARY INFORMATION

1. SCF for a fragment with defect

As a first step to this embedding procedure, a defectless HF calculation is done. The position of the atoms in the defective structure are given as ghost atoms as place holders, each having just one very narrow ($\alpha = 10000000$) s-type GTO as a basis function (ghost atoms without AOs are not allowed in Crystal). In case of the ghost and initial atom coinciding (e.g. in substitution defects), the former is shifted by a very small distance (e.g. 0.00000001) with respect to the latter, as otherwise the HF calculation cannot be carried out. The converged HF orbitals from this calculation are then localized [142]. Furthermore the electrostatic potential is calculated at the new positions the defect's atoms to be used in expression (12). Then, the new atoms are populated with the basis functions using the dual basis technique. The Fock matrix, corresponding to this extended basis set, is built with the density matrix from the initial HF. All these calculations are performed with the Crystal code.

After these steps the fragment is defined on the side of the Cryscor code in terms of the following quantities:

- The initial occupied orbitals of the fragment: $\{i \in \text{frag}\}$
- Atoms that are removed in the defect formation: $\{K \in \text{frag}\}$
- Atoms that are added in the defect formation: $\{K' \in \text{frag}\}$
- The atoms that serve as centers for the fragment's AOs: $\{\mu'\}$

With this the fragment AOs μ' are constructed according to eq. (8).

The next step in the calculation is evaluation of the 2- and 3-index integrals: $(P|Q)$, $(\mu'\nu'|P)$, $(i\mu'|P)$ and $(ii|P)$, where the indices P and Q denote the fitting functions. For evaluation of these integrals the periodic local density fitting machinery of the Cryscor code[15] is used, as described in Ref. [124]. The fit domain is chosen to be universal, coinciding with the atomic fragment for the μ' AOs, such that the one-term robust fitting can be employed.

Next, the 3-index intermediates $B_{\mu'\nu'}^P$, $B_{i\mu'}^P$, B_{ii}^P are calculated according to eq. (13). These intermediates are first used to calculate the Coulomb and exchange matrix elements subtracted from the periodic Fock matrix to evaluate the fragment's one-electron Hamiltonian $h^{\text{frozen frag}}$ (1) in the basis μ' :

$$J_{\mu'\nu'} = \sum_P B_{\mu'\nu'}^P \sum_i B_{ii}^P, \quad (14)$$

$$K_{\mu',\nu'} = \sum_{Pi} B_{i\mu'}^P B_{i\nu'}^P. \quad (15)$$

Further, adding the one-electron integrals to $h_{\mu'\nu'}^{\text{frozen frag}}$ yields $h_{\mu'\nu'}^{\text{defect}}$ according to (9).

In the SCF cycles the quantity $B_{\mu'\nu'}^P$ is used for the actual defective fragment's Coulomb and exchange contributions

$$J_{\mu'\nu'}^{\text{defect}} = \sum_P B_{\mu'\nu'}^P \sum_{\rho'\sigma'} B_{\rho'\sigma'}^P D_{\rho'\sigma'} \quad (16)$$

$$K_{\mu',\nu'}^{\text{defect}} = \sum_P B_{i\mu'}^P B_{i\nu'}^P \quad (17)$$

to the fragment Fock matrix

$$F_{\mu'\nu'}^{\text{defect}} = h_{\mu'\nu'}^{\text{defect}} + 2J_{\mu'\nu'}^{\text{defect}} - K_{\mu',\nu'}^{\text{defect}}. \quad (18)$$

Here $D_{\rho'\sigma'}$ is the density matrix

$$D_{\mu'\nu'} = 2 \sum_{i'} C_{\mu'i'} C_{\nu'i'}, \quad (19)$$

$B_{i'\nu'}^P$ is the half transformed intermediate

$$B_{i'\nu'}^P = \sum_{\mu'} B_{\mu'\nu'}^P C_{\mu'i'}, \quad (20)$$

and $C_{\mu'i'}$ are the orbital expansion coefficients in the fragment basis. The HF energy is evaluated via the expressions (11) and (12). The SCF is accelerated using direct inversion of the iterative subspace (DIIS).[143, 144]

After the SCF has converged, one can readily get to canonical post-HF treatment via the FCIDUMP[125] interface. For this, we assemble the 4-index integrals from the 3-index quantities $B_{\mu'\nu'}^P$ of eq. (13) transformed to the basis of active orbitals r', s', \dots

$$(r's'|t'u') = \sum_P B_{r's'}^P B_{t'u'}^P. \quad (21)$$

2. Size-intensivity of the energy differences

Although expression (11) for the fragment HF energy is not strictly size-extensive, it possesses a more important quantity – asymptotic size-intensivity for the energy differences. Below, we demonstrate this.

Fragment nuclei

Firstly we focus on the nuclei. Consider two systems A and B that deviate from each other by the position and/or type of some atoms in the fragment. For example A and B could be the system with and without defect. The fragment nuclei that are the same in both A and B we denote as “fixed” ($K' \in \text{fixed}$), while the ones that differ in A and B we mark by the corresponding system index: $K'_A \in A$ and $K'_B \in B$. The energy difference $\Delta E_{\text{HF}}^{\text{defect}} = E_{\text{HF}}^{\text{defect}}(A) - E_{\text{HF}}^{\text{defect}}(B)$ will then be:

$$\begin{aligned}
\Delta E_{\text{HF}}^{\text{defect}} = & 2 \sum_{i'_A \in \text{frag}} \left\langle i'_A \left| -\frac{1}{2} \nabla^2 \right| i'_A \right\rangle - 2 \sum_{i'_B \in \text{frag}} \left\langle i'_B \left| -\frac{1}{2} \nabla^2 \right| i'_B \right\rangle \\
& - 2 \sum_{i'_A \in \text{frag}} \left[\left\langle i'_A \left| \sum_{K' \in \text{fixed}} \frac{Z_{K'}}{|\mathbf{r} - \mathbf{R}_{K'}|} \right| i'_A \right\rangle + \left\langle i'_A \left| \sum_{K \notin \text{frag}} \frac{Z_K}{|\mathbf{r} - \mathbf{R}_K|} \right| i'_A \right\rangle \right] \\
& + 2 \sum_{i'_B \in \text{frag}} \left[\left\langle i'_B \left| \sum_{K' \in \text{fixed}} \frac{Z_{K'}}{|\mathbf{r} - \mathbf{R}_{K'}|} \right| i'_B \right\rangle + \left\langle i'_B \left| \sum_{K \notin \text{frag}} \frac{Z_K}{|\mathbf{r} - \mathbf{R}_K|} \right| i'_B \right\rangle \right] \\
& - 2 \sum_{i'_A \in \text{frag}} \left\langle i'_A \left| \sum_{K'_A \in A} \frac{Z_{K'_A}}{|\mathbf{r} - \mathbf{R}_{K'_A}|} \right| i'_A \right\rangle + 2 \sum_{i'_B \in \text{frag}} \left\langle i'_B \left| \sum_{K'_B \in B} \frac{Z_{K'_B}}{|\mathbf{r} - \mathbf{R}_{K'_B}|} \right| i'_B \right\rangle \\
& + \sum_{i'_A \in \text{frag}} \sum_{j \notin \text{frag}} [4(i'_A i'_A | j j) - 2(i'_A j | j i'_A)] - \sum_{i'_B \in \text{frag}} \sum_{j \notin \text{frag}} [4(i'_B i'_B | j j) - 2(i'_B j | j i'_B)] \\
& + \frac{1}{2} \sum_{i'_A \in \text{frag}} \sum_{j'_A \in \text{frag}} [4(i'_A i'_A | j'_A j'_A) - 2(i'_A j'_A | j'_A i'_A)] \\
& - \frac{1}{2} \sum_{i'_B \in \text{frag}} \sum_{j'_B \in \text{frag}} [4(i'_B i'_B | j'_B j'_B) - 2(i'_B j'_B | j'_B i'_B)] \\
& + \sum_{L' \in \text{fixed}} \sum_{K'_A \in A} ' \frac{Z_{L'} Z_{K'_A}}{|\mathbf{R}_{L'} - \mathbf{R}_{K'_A}|} - \sum_{L' \in \text{fixed}} \sum_{K'_B \in B} ' \frac{Z_{L'} Z_{K'_B}}{|\mathbf{R}_{L'} - \mathbf{R}_{K'_B}|} \\
& + \frac{1}{2} \sum_{K'_A \in A} \sum_{L'_A \in A} ' \frac{Z_{K'_A} Z_{L'_A}}{|\mathbf{R}_{K'_A} - \mathbf{R}_{L'_A}|} - \frac{1}{2} \sum_{K'_B \in B} \sum_{L'_B \in B} ' \frac{Z_{K'_B} Z_{L'_B}}{|\mathbf{R}_{K'_B} - \mathbf{R}_{L'_B}|} \\
& - 2 \sum_{i \notin \text{frag}} \left\langle i \left| \sum_{K'_A \in A} \frac{Z_{K'_A}}{|\mathbf{r} - \mathbf{R}_{K'_A}|} \right| i \right\rangle + 2 \sum_{i \notin \text{frag}} \left\langle i \left| \sum_{K'_B \in B} \frac{Z_{K'_B}}{|\mathbf{r} - \mathbf{R}_{K'_B}|} \right| i \right\rangle \\
& + \sum_{L \notin \text{frag}} \sum_{K'_A \in A} \frac{Z_L Z_{K'_A}}{|\mathbf{R}_L - \mathbf{R}_{K'_A}|} - \sum_{L \notin \text{frag}} \sum_{K'_B \in B} \frac{Z_L Z_{K'_B}}{|\mathbf{R}_L - \mathbf{R}_{K'_B}|}. \tag{22}
\end{aligned}$$

The fixed atoms ($K' \in \text{fixed}$ or $L' \in \text{fixed}$) and environment atoms ($K \notin \text{frag}$ or $L \notin \text{frag}$) appear in the same expression: terms 3 and 4, terms 5 and 6, terms 13 and 19, and terms 14 and 20. This shows that $\Delta E_{\text{HF}}^{\text{defect}}$ does not depend on whether the “fixed” nuclei are included in the fragment or in the environment. Even though an inclusion of a nucleus in a fragment does generally affect the fragments total HF energy, the energy difference will remain the same unless this nuclei has a different relative position/type in the respective systems. In other words the energy difference $\Delta E_{\text{HF}}^{\text{frag}}$ is size-intensive with respect to expansion of the nuclei set beyond the explicitly manipulated ones.

Therefore in practical calculations, the summations

over the fragment nuclei K and K' in eqs. (9) or (11) do not need to be performed over the “fixed” ones.

Fragment electrons

Now let us assume that our fragment is large enough that a certain part of the fragment’s localized occupied orbitals at the boundary of the fragment does not feel the presence of the defect and remain the same as in the initial bulk calculation, we will denote such orbitals as “bulk”: $i' \in \text{bulk}$, in contrast to the orbitals $i'_A \in \text{frag}$ and $i'_B \in \text{frag}$. Then the energy difference $\Delta E_{\text{HF}}^{\text{defect}}$ will take the form:

$$\begin{aligned}
\Delta E_{\text{HF}}^{\text{defect}} = & 2 \sum_{i'_A \in \text{frag}} \left\langle i'_A \left| -\frac{1}{2} \nabla^2 \right| i'_A \right\rangle - 2 \sum_{i'_B \in \text{frag}} \left\langle i'_B \left| -\frac{1}{2} \nabla^2 \right| i'_B \right\rangle \\
& - 2 \sum_{i'_A \in \text{frag}} \left\langle i'_A \left| \sum_{K \notin \text{frag}} \frac{Z_K}{|\mathbf{r} - \mathbf{R}_K|} \right| i'_A \right\rangle + 2 \sum_{i'_B \in \text{frag}} \left\langle i'_B \left| \sum_{K \notin \text{frag}} \frac{Z_K}{|\mathbf{r} - \mathbf{R}_K|} \right| i'_B \right\rangle \\
& - 2 \sum_{i'_A \in \text{frag}} \left\langle i'_A \left| \sum_{K'_A \in A} \frac{Z_{K'_A}}{|\mathbf{r} - \mathbf{R}_{K'_A}|} \right| i'_A \right\rangle + 2 \sum_{i'_B \in \text{frag}} \left\langle i'_B \left| \sum_{K'_B \in B} \frac{Z_{K'_B}}{|\mathbf{r} - \mathbf{R}_{K'_B}|} \right| i'_B \right\rangle \\
& - 2 \sum_{i' \in \text{bulk}} \left\langle i' \left| \sum_{K'_A \in A} \frac{Z_{K'_A}}{|\mathbf{r} - \mathbf{R}_{K'_A}|} \right| i' \right\rangle + 2 \sum_{i' \in \text{bulk}} \left\langle i' \left| \sum_{K'_B \in B} \frac{Z_{K'_B}}{|\mathbf{r} - \mathbf{R}_{K'_B}|} \right| i' \right\rangle \\
& + \sum_{i'_A \in \text{frag}} \sum_{j \notin \text{frag}} [4(i'_A i'_A | j j) - 2(i'_A j | j i'_A)] - \sum_{i'_B \in \text{frag}} \sum_{j \notin \text{frag}} [4(i'_B i'_B | j j) - 2(i'_B j | j i'_B)] \\
& + \frac{1}{2} \sum_{i'_A \in \text{frag}} \sum_{j'_A \in \text{frag}} [4(i'_A i'_A | j'_A j'_A) - 2(i'_A j'_A | j'_A i'_A)] \\
& - \frac{1}{2} \sum_{i'_B \in \text{frag}} \sum_{j'_B \in \text{frag}} [4(i'_B i'_B | j'_B j'_B) - 2(i'_B j'_B | j'_B i'_B)] \\
& + \sum_{i'_A \in \text{frag}} \sum_{j' \in \text{bulk}} [4(i'_A i'_A | j' j') - 2(i'_A j' | j' i'_A)] - \sum_{i'_B \in \text{frag}} \sum_{j' \in \text{bulk}} [4(i'_B i'_B | j' j') - 2(i'_B j' | j' i'_B)] \\
& + \frac{1}{2} \sum_{K'_A \in A} \sum_{L'_A \in A} \frac{Z_{K'_A} Z_{L'_A}}{|\mathbf{R}_{K'_A} - \mathbf{R}_{L'_A}|} - \frac{1}{2} \sum_{K'_B \in B} \sum_{L'_B \in B} \frac{Z_{K'_B} Z_{L'_B}}{|\mathbf{R}_{K'_B} - \mathbf{R}_{L'_B}|} \\
& - 2 \sum_{i \notin \text{frag}} \left\langle i \left| \sum_{K'_A \in A} \frac{Z_{K'_A}}{|\mathbf{r} - \mathbf{R}_{K'_A}|} \right| i \right\rangle + 2 \sum_{i \notin \text{frag}} \left\langle i \left| \sum_{K'_B \in B} \frac{Z_{K'_B}}{|\mathbf{r} - \mathbf{R}_{K'_B}|} \right| i \right\rangle \\
& + \sum_{L \notin \text{frag}} \sum_{K'_A \in A} \frac{Z_L Z_{K'_A}}{|\mathbf{R}_L - \mathbf{R}_{K'_A}|} - \sum_{L \notin \text{frag}} \sum_{K'_B \in B} \frac{Z_L Z_{K'_B}}{|\mathbf{R}_L - \mathbf{R}_{K'_B}|}. \tag{23}
\end{aligned}$$

Again $\Delta E_{\text{HF}}^{\text{frag}}$ becomes insensitive to inclusion of the bulk region of the fragment into environment (compare the terms 7 and 17, terms 8 and 18, terms 13 and 9, and terms 14 and 10). It shows that asymptotically $\Delta E_{\text{HF}}^{\text{frag}}$ is size-intensive with respect to expansion of the fragment.

3. Computational details: Bond dissociation in fluorographane

The initial structure of graphane was optimized at the periodic B3LYP-D3 level[145, 146] with the pob-TZVP-rev2 basis[147] For each fragment we performed a single-point periodic HF calculation on this pristine graphane with primitive unit cell, with an addition of a ghost atom at the new position of the carbon and fluorine atoms of the defect C-F bond. The equilibrium C-F bond length and position of this carbon atom was optimized also with periodic B3LYP-D3 on a 3 by 3 supercell with all other atoms frozen. Implementation of fragment gradients will be addressed in a future publication such that DFT ge-

ometry optimizations of supercells will not be required. For each C-F bond length considered the position of the carbon atom was not re-optimized. Formation of the defect represented therefore removal of carbon and a hydrogen atom and addition of carbon (at the new position) and a fluorine atom (corresponding to the varied bond length). For the choice of embedded fragment, we selected the same 14 atoms as in Refs. [104, 106]: one fluorine atom, ten carbon atoms, and three hydrogen atoms, as is shown in Figure 1. After the fragment's HF, we performed post-HF calculations via the FCIDUMP interface, using a variety of single- and multireference methods. For the density fitting, we used the fitting basis set optimized for MP2/cc-pVTZ calculations.[148]

* denis.usvyat@hu-berlin.de

[1] C. Pisani, L. Maschio, S. Casassa, M. Halo, M. Schütz, and D. Usvyat, *J. Comput. Chem.* **29**, 2113 (2008).

- [2] D. Usvyat, L. Maschio, C. Pisani, and M. Schütz, *Z. Phys. Chem.* **224**, 441 (2010).
- [3] D. Usvyat, L. Maschio, and M. Schütz, *J. Chem. Phys.* **143**, 102805 (2015).
- [4] J. McClain, Q. Sun, G. K.-L. Chan, and T. C. Berkelbach, *J. Chem. Theory Comput.* **13**, 1209 (2017).
- [5] T. Gruber, K. Liao, T. Tsatsoulis, F. Hummel, and A. Grüneis, *JPhys. Rev. X* **8**, 021043 (2018).
- [6] J. J. Shepherd, A. Grüneis, G. H. Booth, G. Kresse, and A. Alavi, *Phys. Rev. B* **86**, 035111 (2012).
- [7] M. Marsman, A. Grüneis, J. Paier, and G. Kresse, *Journal of Chemical Physics* **130** (2009), 10.1063/1.3126249.
- [8] G. H. Booth, A. Grüneis, G. Kresse, and A. Alavi, *Nature* **493** (2013), 10.1038/nature11770.
- [9] A. Grüneis, J. J. Shepherd, A. Alavi, D. P. Tew, and G. H. Booth, *Journal of Chemical Physics* **139** (2013), 10.1063/1.4818753.
- [10] M. D. Ben, J. Hutter, and J. Vandevondele, *Journal of Chemical Physics* **143** (2015), 10.1063/1.4919238.
- [11] M. D. Ben, J. Hutter, and J. Vandevondele, *Journal of Chemical Theory and Computation* **9** (2013), 10.1021/ct4002202.
- [12] A. Grüneis, *Journal of Chemical Physics* **143** (2015), 10.1063/1.4928645.
- [13] V. V. Rybkin and J. Vandevondele, *Journal of Chemical Theory and Computation* **12** (2016), 10.1021/acs.jctc.6b00015.
- [14] G. H. Booth, T. Tsatsoulis, G. K. L. Chan, and A. Grüneis, *Journal of Chemical Physics* **145** (2016), 10.1063/1.4961301.
- [15] C. Pisani, M. Schütz, S. Casassa, D. Usvyat, L. Maschio, M. Lorenz, and A. Erba, “Cryscor: A program for the post-hartree-fock treatment of periodic systems,” (2012).
- [16] K. Liao, T. Schraivogel, H. Luo, D. Kats, and A. Alavi, *Physical Review Research* **3** (2021), 10.1103/physrevresearch.3.033072.
- [17] X. Wang and T. C. Berkelbach, *Journal of Chemical Theory and Computation* **16**, 3095–3103 (2020).
- [18] V. A. Neufeld and T. C. Berkelbach, *Physical Review Letters* **131** (2023), 10.1103/physrevlett.131.186402.
- [19] S. J. Bintrim, T. C. Berkelbach, and H.-Z. Ye, *Journal of Chemical Theory and Computation* **18**, 5374–5381 (2022).
- [20] N. Masios, A. Irmeler, T. Schäfer, and A. Grüneis, *Physical Review Letters* **131** (2023), 10.1103/physrevlett.131.186401.
- [21] H. Stoll, *Phys. Rev. B* **46**, 6700 (1992).
- [22] H. Stoll, *Chemical Physics Letters* **191** (1992), 10.1016/0009-2614(92)85587-Z.
- [23] A. Hermann and P. Schwerdtfeger, *Physical Review Letters* **101** (2008), 10.1103/PhysRevLett.101.183005.
- [24] “The method of increments—a wavefunction-based correlation method for extended systems,” (2020).
- [25] B. Paulus, *Phys. Rep.* **428**, 1 (2006).
- [26] C. Müller and B. Paulus, *Physical Chemistry Chemical Physics* **14** (2012), 10.1039/c2cp24020c.
- [27] C. Tuma and J. Sauer, *Phys. Chem. Chem. Phys.* **8**, 3955 (2006).
- [28] S. J. Nolan, M. J. Gillan, D. Alfè, N. L. Allan, and F. R. Manby, *Phys. Rev. B* **80**, 165109 (2009).
- [29] J. Yang, W. Hu, D. Usvyat, D. Matthews, M. Schütz, and G. K.-L. Chan, *Science* **345**, 6197 (2014).
- [30] C. Müller and D. Usvyat, *J. Chem. Theory Comput.* **9**, 5590 (2013).
- [31] D. Usvyat, *J. Chem. Phys.* **143**, 104704 (2015).
- [32] T. Tsatsoulis, F. Hummel, D. Usvyat, M. Schütz, G. H. Booth, S. S. Binnie, M. J. Gillan, D. Alfe, A. Michaelides, and A. Grüneis, *J. Chem. Phys.* **146**, 204108 (2017).
- [33] M. Schütz, L. Maschio, A. J. Karttunen, and D. Usvyat, *J. Phys. Chem. Lett.* **8**, 1290 (2017).
- [34] M. Alessio, F. A. Bischoff, and J. Sauer, *Phys. Chem. Chem. Phys.* **20**, 9760 (2018).
- [35] M. Alessio, D. Usvyat, and J. Sauer, *J. Chem. Theory Comput.* **20**, 1329 (2019).
- [36] S. Wen and G. J. Beran, *Journal of Chemical Theory and Computation* **7** (2011), 10.1021/ct200541h.
- [37] J. Li, O. Sode, G. A. Voth, and S. Hirata, *Nature Communications* **4** (2013), 10.1038/ncomms3647.
- [38] Q. Sun and G. K. L. Chan, *Accounts of Chemical Research* **49** (2016), 10.1021/acs.accounts.6b00356.
- [39] C. Pisani, *Physical Review B* **17**, 3143–3153 (1978).
- [40] C. Pisani, R. Dovesi, and P. Carosso, *Physical Review B* **20**, 5345–5357 (1979).
- [41] P. J. Bygrave, N. L. Allan, and F. R. Manby, *J. Chem. Phys.* **137**, 164102 (2012).
- [42] F. R. Manby, M. Stella, J. D. Goodpaster, and T. F. Miller, *Journal of Chemical Theory and Computation* **8** (2012), 10.1021/ct300544e.
- [43] G. Knizia and G. K.-L. Chan, *Phys. Rev. Lett.* **109**, 186404 (2012).
- [44] G. Knizia and G. K. L. Chan, *Journal of Chemical Theory and Computation* **9** (2013), 10.1021/ct301044e.
- [45] T. N. Lan, A. A. Kananenka, and D. Zgid, *Journal of Chemical Physics* **143** (2015), 10.1063/1.4938562.
- [46] N. Govind, Y. A. Wang, A. J. D. Silva, and E. A. Carter, *Chemical Physics Letters* **295** (1998), 10.1016/S0009-2614(98)00939-7.
- [47] T. Klüner, N. Govind, Y. A. Wang, and E. A. Carter, *Journal of Chemical Physics* **116** (2002), 10.1063/1.1420748.
- [48] K. Jug and T. Bredow, “Models for the treatment of crystalline solids and surfaces,” (2004).
- [49] P. Huang and E. A. Carter, *Journal of Chemical Physics* **125** (2006), 10.1063/1.2336428.
- [50] C. Müller, B. Herschend, K. Hermansson, and B. Paulus, *Journal of Chemical Physics* **128** (2008), 10.1063/1.2921799.
- [51] P. Huang and E. A. Carter, *Annual Review of Physical Chemistry* **59** (2008), 10.1146/annurev.physchem.59.032607.093528.
- [52] T. A. Barnes, J. D. Goodpaster, F. R. Manby, and T. F. Miller, *Journal of Chemical Physics* **139** (2013), 10.1063/1.4811112.
- [53] A. D. Boese and J. Sauer, *Phys. Chem. Chem. Phys.* **15**, 16481 (2013).
- [54] J. D. Goodpaster, T. A. Barnes, F. R. Manby, and T. F. Miller, *Journal of Chemical Physics* **140** (2014), 10.1063/1.4864040.
- [55] C. R. Jacob and J. Neugebauer, “Subsystem density-functional theory,” (2014).
- [56] M. E. Fornace, J. Lee, K. Miyamoto, F. R. Manby, and T. F. Miller, “Erratum: Embedded mean-field theory (j. chem. theory comput. (2015) 11:2 (568-580) doi: 10.1021/ct5011032),” (2015).

- [57] F. Libisch, M. Marsman, J. Burgdörfer, and G. Kresse, *Journal of Chemical Physics* **147** (2017), 10.1063/1.4993795.
- [58] D. V. Chulhai and J. D. Goodpaster, *Journal of Chemical Theory and Computation* **14** (2018), 10.1021/acs.jctc.7b01154.
- [59] Z. H. Cui, T. Zhu, and G. K. L. Chan, *Journal of Chemical Theory and Computation* **16** (2020), 10.1021/acs.jctc.9b00933.
- [60] T. Zhu, Z.-H. Cui, and G. K.-L. Chan, *Journal of Chemical Theory and Computation* **16**, 141–153 (2019).
- [61] H. Q. Pham, M. R. Hermes, and L. Gagliardi, *Journal of Chemical Theory and Computation* **16** (2020), 10.1021/acs.jctc.9b00939.
- [62] S. Wouters, C. A. Jiménez-Hoyos, Q. Sun, and G. K. Chan, *Journal of Chemical Theory and Computation* **12** (2016), 10.1021/acs.jctc.6b00316.
- [63] A. Mitra, H. Q. Pham, R. Pandharkar, M. R. Hermes, and L. Gagliardi, *Journal of Physical Chemistry Letters* **12** (2021), 10.1021/acs.jpcclett.1c03229.
- [64] B. Hégyely, P. R. Nagy, G. G. Ferenczy, and M. Kállay, *Journal of Chemical Physics* **145** (2016), 10.1063/1.4960177.
- [65] N. Sheng, C. Vorwerk, M. Govoni, and G. Galli, *Journal of Chemical Theory and Computation* **18** (2022), 10.1021/acs.jctc.2c00240.
- [66] C. Vorwerk, N. Sheng, M. Govoni, B. Huang, and G. Galli, *Nature Computational Science* **2** (2022), 10.1038/s43588-022-00279-0.
- [67] M. T. Wachter-Lehn, K. Fink, and S. Höfener, *The Journal of Chemical Physics* **157** (2022), 10.1063/5.0102267.
- [68] A. Georges and G. Kotliar, *Physical Review B* **45**, 6479–6483 (1992).
- [69] A. Georges, G. Kotliar, W. Krauth, and M. J. Rozenberg, *Reviews of Modern Physics* **68**, 13–125 (1996).
- [70] G. Kotliar, S. Y. Savrasov, K. Haule, V. S. Oudovenko, O. Parcollet, and C. A. Marianetti, *Reviews of Modern Physics* **78**, 865–951 (2006).
- [71] D. Vollhardt, *Annalen der Physik* **524**, 1–19 (2011).
- [72] J. M. Callahan, M. F. Lange, and T. C. Berkelbach, *The Journal of Chemical Physics* **154** (2021), 10.1063/5.0049890.
- [73] M. Welborn, T. Tsuchimochi, and T. Van Voorhis, *The Journal of Chemical Physics* **145** (2016), 10.1063/1.4960986.
- [74] M. Ditte, M. Barborini, L. Medrano Sandonas, and A. Tkatchenko, *Physical Review Letters* **131** (2023), 10.1103/physrevlett.131.228001.
- [75] M. Nusspickel and G. H. Booth, *Physical Review X* **12** (2022), 10.1103/physrevx.12.011046.
- [76] L. Lacombe and N. T. Maitra, *Physical Review Letters* **124** (2020), 10.1103/physrevlett.124.206401.
- [77] A. Wasserman and M. Pavanello, *International Journal of Quantum Chemistry* **120** (2020), 10.1002/qua.26495.
- [78] C. Mejuto-Zaera, *Faraday Discussions* (2024), 10.1039/d4fd00053f.
- [79] N. Lanatà, *Physical Review B* **108** (2023), 10.1103/physrevb.108.235112.
- [80] D. Sénéchal, D. Perez, and M. Pioro-Ladrière, *Physical Review Letters* **84**, 522–525 (2000).
- [81] M. S. Frank, T.-H. Lee, G. Bhattacharyya, P. K. H. Tsang, V. L. Quito, V. Dobrosavljević, O. Christiansen, and N. Lanatà, *Physical Review B* **104** (2021), 10.1103/physrevb.104.1081103.
- [82] N. Lanatà, Y. Yao, X. Deng, V. Dobrosavljević, and G. Kotliar, *Physical Review Letters* **118** (2017), 10.1103/physrevlett.118.126401.
- [83] G. Rohringer, H. Hafermann, A. Toschi, A. Katanin, A. Antipov, M. Katsnelson, A. Lichtenstein, A. Rubtsov, and K. Held, *Reviews of Modern Physics* **90** (2018), 10.1103/revmodphys.90.025003.
- [84] G. Kotliar and A. E. Ruckenstein, *Physical Review Letters* **57**, 1362–1365 (1986).
- [85] T. Ayral, T.-H. Lee, and G. Kotliar, *Physical Review B* **96** (2017), 10.1103/physrevb.96.235139.
- [86] A. B. Georgescu and S. Ismail-Beigi, *Physical Review B* **92** (2015), 10.1103/physrevb.92.235117.
- [87] S. Biermann, F. Aryasetiawan, and A. Georges, *Physical Review Letters* **90** (2003), 10.1103/physrevlett.90.086402.
- [88] T. Zhu and G. K.-L. Chan, *Physical Review X* **11** (2021), 10.1103/physrevx.11.021006.
- [89] N. Lanatà, Y. Yao, C.-Z. Wang, K.-M. Ho, and G. Kotliar, *Physical Review X* **5** (2015), 10.1103/physrevx.5.011008.
- [90] P. V. Sriluckshmy, M. Nusspickel, E. Fertitta, and G. H. Booth, *Physical Review B* **103** (2021), 10.1103/physrevb.103.085131.
- [91] E. Fertitta and G. H. Booth, *Physical Review B* **98** (2018), 10.1103/physrevb.98.235132.
- [92] J. Tilly, P. V. Sriluckshmy, A. Patel, E. Fontana, I. Rungger, E. Grant, R. Anderson, J. Tennyson, and G. H. Booth, *Physical Review Research* **3** (2021), 10.1103/physrevresearch.3.033230.
- [93] G. H. Booth and G. K.-L. Chan, *Physical Review B* **91** (2015), 10.1103/physrevb.91.155107.
- [94] L. O. Jones, M. A. Mosquera, G. C. Schatz, and M. A. Ratner, *Journal of the American Chemical Society* **142**, 3281–3295 (2020).
- [95] A. Shee, F. M. Faulstich, B. Whaley, L. Lin, and M. Head-Gordon, “A static quantum embedding scheme based on coupled cluster theory,” (2024).
- [96] L. Lin and M. Lindsey, *Communications on Pure and Applied Mathematics* **75**, 2033–2068 (2021).
- [97] M. A. Mosquera, L. O. Jones, M. A. Ratner, and G. C. Schatz, *International Journal of Quantum Chemistry* **120** (2020), 10.1002/qua.26184.
- [98] H. Ma, N. Sheng, M. Govoni, and G. Galli, *Journal of Chemical Theory and Computation* **17**, 2116–2125 (2021).
- [99] U. Birkenheuer, P. Fulde, and H. Stoll, *Theoretical Chemistry Accounts* **116**, 398–403 (2006).
- [100] L. Hozoi, U. Birkenheuer, H. Stoll, and P. Fulde, *New Journal of Physics* **11**, 023023 (2009).
- [101] A. Stoyanova, A. O. Mitrushchenkov, L. Hozoi, H. Stoll, and P. Fulde, *Physical Review B* **89** (2014), 10.1103/physrevb.89.235121.
- [102] O. Masur, M. Schütz, L. Maschio, and D. Usvyat, *J. Chem. Theory Comput.* **12**, 5145 (2016).
- [103] D. Usvyat, L. Maschio, and M. Schütz, *WIREs: Comput. Mol. Sci.* **8**, e1357 (2018).
- [104] H. H. Lin, L. Maschio, D. Kats, D. Usvyat, and T. Heine, *J. Chem. Theory Comput.* **16**, 7100 (2020).
- [105] T. Schäfer, F. Libisch, G. Kresse, and A. Grüneis, *J. Chem. Phys.* **154**, 011101 (2021).
- [106] E. M. Christlmaier, D. Kats, A. Alavi, and D. Usvyat, *J. Chem. Phys.* **156**, 074109 (2022).

- [107] B. T. G. Lau, G. Knizia, and T. C. Berkelbach, *J. Phys. Chem. Lett.* **12**, 1104 (2021).
- [108] C. Freysoldt, J. Neugebauer, and C. G. Van de Walle, *Phys. Rev. Lett.* **102**, 016402 (2009).
- [109] G. Makov and M. C. Payne, *Phys. Rev. B* **51**, 4014 (1995).
- [110] J. Neugebauer and M. Scheffler, *Phys. Rev. B* **46**, 16067 (1992).
- [111] “Monopole Dipole and Quadrupole Corrections - VASP Wiki — vasp.at,” https://www.vasp.at/wiki/index.php/Monopole_Dipole_and_Quadrupole_Corrections, [Accessed 28-05-2024].
- [112] C. Sousa and F. Illas, *The Journal of Chemical Physics* **115**, 1435–1439 (2001).
- [113] E. D. Larsson, M. Krośnicki, and V. Veryazov, *Chemical Physics* **562**, 111549 (2022).
- [114] N. A. Bogdanov, J. van den Brink, and L. Hozoi, *Physical Review B* **84** (2011), 10.1103/physrevb.84.235146.
- [115] N. A. Bogdanov, V. M. Katukuri, H. Stoll, J. van den Brink, and L. Hozoi, *Physical Review B* **85** (2012), 10.1103/physrevb.85.235147.
- [116] N. A. Bogdanov, G. Li Manni, S. Sharma, O. Gunnarsson, and A. Alavi, *Nature Physics* **18**, 190–195 (2021).
- [117] V. M. Katukuri, N. A. Bogdanov, O. Weser, J. van den Brink, and A. Alavi, *Physical Review B* **102** (2020), 10.1103/physrevb.102.241112.
- [118] V. M. Katukuri, N. A. Bogdanov, and A. Alavi, *Frontiers in Physics* **10** (2022), 10.3389/fphy.2022.836784.
- [119] J. Chen, N. A. Bogdanov, D. Usvyat, W. Fang, A. Michaelides, and A. Alavi, *J. Chem. Phys.* **153**, 204704 (2020).
- [120] T. Petersen, U. K. Rößler, and L. Hozoi, *Communications Physics* **5** (2022), 10.1038/s42005-022-00979-z.
- [121] G. H. Booth, A. J. W. Thom, and A. Alavi, *The Journal of Chemical Physics* **131** (2009), 10.1063/1.3193710.
- [122] G. K.-L. Chan and S. Sharma, *Annual Review of Physical Chemistry* **62**, 465–481 (2011).
- [123] A. Erba, J. K. Desmarais, S. Casassa, B. Civalleri, L. Donà, I. J. Bush, B. Searle, L. Maschio, L. Edith-Daga, A. Cossard, C. Ribaldone, E. Ascriczzi, N. L. Marana, J.-P. Flament, and B. Kirtman, *Journal of Chemical Theory and Computation* **19**, 6891–6932 (2022).
- [124] D. Usvyat, *J. Chem. Phys.* **139**, 194101 (2013).
- [125] P. J. Knowles and N. C. Handy, *Comput. Phys. Commun.* **54**, 75 (1989).
- [126] H.-J. Werner, P. J. Knowles, F. R. Manby, J. A. Black, K. Doll, A. Heßelmann, D. Kats, A. Köhn, T. Korona, D. A. Kreplin, Q. Ma, T. F. Miller, A. Mitrushchenkov, K. A. Peterson, I. Polyak, G. Rauhut, and M. Sibaeav, *J. Chem. Phys.* **152**, 144107 (2020).
- [127] H. Werner and P. J. Knowles, *The Journal of Chemical Physics* **89**, 5803 (1988), https://pubs.aip.org/aip/jcp/article-pdf/89/9/5803/18973113/5803_1_online.pdf.
- [128] P. J. Knowles and H.-J. Werner, *Chemical Physics Letters* **145**, 514 (1988).
- [129] P. Celani and H.-J. Werner, *The Journal of Chemical Physics* **112**, 5546–5557 (2000).
- [130] D. Kats and F. R. Manby, *The Journal of Chemical Physics* **139** (2013), 10.1063/1.4813481.
- [131] D. Kats, *The Journal of Chemical Physics* **144** (2016), 10.1063/1.4940398.
- [132] D. Kats, *The Journal of Chemical Physics* **141** (2014), 10.1063/1.4892792.
- [133] N. C. Handy, J. A. Pople, M. Head-Gordon, K. Raghavachari, and G. W. Trucks, *Chemical Physics Letters* **164**, 185–192 (1989).
- [134] R. A. Chiles and C. E. Dykstra, *The Journal of Chemical Physics* **74**, 4544–4556 (1981).
- [135] A. J. Cohen, H. Luo, K. Guther, W. Dobrautz, D. P. Tew, and A. Alavi, *The Journal of Chemical Physics* **151** (2019), 10.1063/1.5116024.
- [136] E. M. C. Christlmaier, T. Schraivogel, P. López Ríos, A. Alavi, and D. Kats, *The Journal of Chemical Physics* **159** (2023), 10.1063/5.0154445.
- [137] S. Ismail-Beigi and T. A. Arias, *Physical Review Letters* **82**, 2127–2130 (1999).
- [138] R. Matveeva, S. D. Folkestad, and I.-M. Høyvik, *The Journal of Physical Chemistry A* **127**, 1329–1341 (2023).
- [139] E. Fertitta and G. H. Booth, *The Journal of Chemical Physics* **151** (2019), 10.1063/1.5100290.
- [140] H. D. Cornean, D. Gontier, A. Levitt, and D. Monaco, *Annales Henri Poincaré* **20**, 1367 (2019).
- [141] H. Luo and A. Alavi, *The Journal of Chemical Physics* **157** (2022), 10.1063/5.0101776.
- [142] C. M. Zicovich-Wilson, R. Dovesi, and V. R. Saunders, *J. Chem. Phys.* **115**, 9708 (2001).
- [143] P. Pulay, *Chemical Physics Letters* **73**, 393–398 (1980).
- [144] P. Pulay, *Journal of Computational Chemistry* **3**, 556–560 (1982).
- [145] C. Lee, W. Yang, and R. G. Parr, *Physical Review B* **37**, 785–789 (1988).
- [146] S. Grimme, J. Antony, S. Ehrlich, and H. Krieg, *The Journal of Chemical Physics* **132** (2010), 10.1063/1.3382344.
- [147] D. Vilela Oliveira, J. Laun, M. F. Peintinger, and T. Bredow, *Journal of Computational Chemistry* **40**, 2364–2376 (2019).
- [148] F. Weigend, A. Köhn, and C. Hättig, *J. Chem. Phys.* **116**, 3175 (2002).